Model-based Workflow For Sustainable Production of High-quality Spirits in Packed Column Stills

Simón Díaz-Quezada[1], David I. Wilson[2], and José R. Pérez-Correa[1,*]

[1]Chemical and Bioprocess Engineering Department, School of Engineering, Pontificia Universidad Católica de Chile, Vicuña Mackenna 4860, 7820436, Santiago, Chile.

[2]Industrial Information Control Centre, Auckland University of Technology, 47 Saint Paul Street, Auckland CBD, Auckland 101, New Zealand.

*Corresponding author: J.R. Pérez-Correa (e-mail: jperezc@uc.cl).

Abstract

This study addresses the water scarcity issue in Chilean distilleries by developing a model-based engineering workflow. Prolonged droughts, likely linked to global warming, have exacerbated this problem. The primary challenge is to maintain high-quality spirits while reducing cooling water and energy use during batch distillation in packed columns. Using mass and energy balances, this process is modeled as a partial differential algebraic equation (PDAE) system. Our workflow includes mechanistic modeling, disturbance modeling, multiobjective optimization, model predictive control, and Monte Carlo simulations. Our findings show that cooling water consumption can be reduced by up to 35% and energy consumption by up to 14.4% while maintaining product quality. The proposed system is robust against operational disturbances and model mismatch, ensuring consistent distillate quality. This research demonstrates the integration of model-based optimization and control strategies in batch distillation processes and can be replicated in other fruit wine distillation processes for improved sustainability.

Keywords: Fruit wine, batch distillation, multiobjective optimization, partial differential algebraic equation systems, water consumption.

1. Introduction

Producing high-quality spirits with unique flavors and aromas in batch column stills is a major concern in the rapidly growing fruit wine industry (Holds, 2023). The complex distillation process is mainly influenced by the fermented fruit juice used and the specific operating recipe applied to achieve the desired aroma profile (Sacher et al., 2017), which determines the expected quality and the respective typification that differentiates it from other distillates (Agosin et al., 2000). However, this process also raises environmental concerns due to the extensive use of cooling water and energy (Barbosa et al., 2018).

Studying environmental impacts and sustainability in wine and spirits production has become increasingly critical. Notably, Martins et al., (2018) achieved a 10 % reduction in solid waste by implementing sustainable practices in winemaking. Similarly, Iannone et al., (2016) reported a significant decrease of 95 % in carbon dioxide emissions by optimizing temperatures utilizing life cycle assessment (LCA) methodologies. Barbosa et al. (2018) highlighted the importance of water reuse and consumption reduction strategies for enhancing winemaking sustainability, especially in regions where climatic variables heavily influence viticulture. Applying scenario simulations in Aspen Plus®, Silva et al., (2017) obtained a 24 % waste reduction by integrating a reboiler into the distillation process. Additionally, Nemeth et al., (2020) demonstrated a 20 % reduction in CO2 emissions and a 30 % improvement in productivity by optimizing the solvent recovery process in batch distillation columns using genetic algorithms to adjust the reflux ratio and stopping criteria in ChemCAD simulations. Becker et al., (2020) proposed that the French spirits industry could achieve carbon neutrality by lowering emissions by 10 % and reducing the weight of bottles. Our research contributes to this growing body of work by further exploring advanced model-based techniques to reproducibly improve the performance and sustainability of fruit wine distillation.

The spirits distillation industry faces two major problems. The first is related to suboptimal operating policies that don't guarantee the quality of the distillate, which is made more difficult by the need to reduce environmental impact and water and energy consumption, highlighting the need for sustainability efforts

(Diwekar et al., 2021; White, 2023). The problem of increasing water scarcity is particularly acute in regions such as northern Chile, a hub for producing pisco, the most traditional and important spirit produced in the country (Muñoz et al., 2020). Moreover, despite the known dependence of the distillate on the process recipe, stills are manually operated, which affects the aroma composition (Arrieta-Garay et al., 2014; Balanuta et al., 2021). As a result, the uncontrolled operations lead to irreproducible distillations (García-Llobodanin et al., 2011; Heller and Einfalt, 2022).

Developing models that can reproduce the sophistication of real fruit wine distillations is essential to advance practical solutions for the spirits industry. The level of sophistication of the model depends on the type of distillation equipment. Copper alembic models are easier to solve because they typically include two stages that can be well represented with a few ordinary differential and algebraic equations. Modeling batch plate columns is more challenging due to the need for an extra stage for each plate, leading to a complex differential algebraic equation (DAE) system requiring specific numerical methods. Batch-packed column distillation units, represented by partial differential algebraic equation (PDAE) systems, are even more complex to model. The modeling of the different types of distillation units using several fruit wines has been extensively studied. The production of pisco from Muscat wine has been modeled in copper alembics (Luna et al., 2019, 2018), batch plate columns (De Lucca et al., 2013; Osorio et al., 2005, 2004), and batch-packed columns (Carvallo et al., 2011; Diaz-Quezada et al., 2022). In addition, copper alembic models have been developed for cachaça (Scanavini et al., 2010; Soares et al., 2019; Tenorio et al., 2023), gin (Hodel et al., 2021), pear wine brandy (Sacher et al., 2013), and slivovitz, a fruit spirit made from damson (Spaho, 2017). Plate column models are available for whiskey (Valderrama et al., 2012) and fruit brandies (Douady et al., 2019; Hodel et al., 2021). These models provide important insights to improve the operation of the respective distillation unit and help better understand how to increase the recovery of specific aromas of a given fermented fruit juice. However, these models are rarely used to optimize the distillation recipe or design control systems to minimize the impact of process variability on product quality, productivity, and sustainability.

In Chemical Engineering, multiobjective optimization (MOO) for batch processes has received considerable attention due to its potential to develop sustainable and efficient operating methods. In particular, Luna et al. (2021) used MOO to design optimal wine distillation recipes, emphasizing energy efficiency while focusing on quality and food safety. Parhi et al. (2019) studied a vapor-compressed distillation column in batch distillation, focusing on energy savings and economic viability based on optimization. Another relevant application of MOO has been in batch processes in the pharmaceutical industry (Sarkar et al., 2006; Sridhar, 2020), focusing on optimal process design for quality improvement. However, an overarching theme in these efforts is the commitment to sustainability, as evidenced by works applied to the design of batch chemical processes based on multiobjective optimization using the MINSOOP algorithm. Using this procedure, Diwekar (2005) and Fu & Diwekar (2004) achieved a 30 % cost reduction, a 15 % efficiency increase, and 10 % reduced emissions in a batch process. A recent review of MOO algorithms and applications in the field of water and environmental sciences was made by Yaghoubzadeh-Bavandpour et al. (2022); they discuss a wide range of algorithms considering swarm intelligence, evolutionary computation, science-based, and human-based. In their review, Yaghoubzadeh-Bavandpour et al. point out that the most applied MOO algorithm in the water and environmental sciences is NSGA-II.

Despite the significant advances in sustainable process systems engineering, most have not been widely adopted in the spirits production industry. Ensuring the reproducibility and applicability of process optimization models in real-world industrial settings is a significant challenge, especially when dealing with time-varying disturbances. Few optimization studies have considered reproducibility in realistic scenarios with time-varying disturbances. Diwekar (2003) enhanced the acetic acid extraction-distillation process by optimizing the recovery ratio and minimizing environmental toxicity under variable conditions and uncertain process parameters. These authors achieved consistent recovery with up to a 90 % reduction in toxicity, highlighting the importance of including variability in the optimization process. While MOO has proven effective for optimizing various objectives in batch processes, selecting the optimal solution from the Pareto front remains challenging. Decision-making methods like TOPSIS are useful for this selection, which is commonly applied for its straightforward approach to balancing conflicting objectives by ranking them using Euclidean distances, as noted in distillation process studies (Krishnan et al., 2023; Luna et al., 2021).

Distilling fermented fruit wines in stills presents significant process control challenges due to the varying operating conditions, unlike continuous processes that mostly operate in steady-state. Adopting automatic

control techniques in the fruit wine distillation industry has been slow despite being successfully applied to many other batch chemical processes (Lopez-Saucedo et al., 2016; Völker et al., 2007). Controllers can be designed and tuned to track optimal trajectories and reject disturbances, reducing the variability between distillations (May-Vázquez et al., 2022). Therefore, these techniques can improve distillation performance, process reproducibility, and disturbance management, aligning with industry sustainability goals (Monroy-Loperena and Alvarez-Ramirez, 2000). The Proportional Integral Controller (PI) with tuning rules based on Internal Model Control (IMC), which is widely adopted in the process industry, is a good and cost-effective option for controlling batch distillation of spirits, as it requires minimal control instrumentation, shows satisfactory performance in most cases and is easy to tune. Typically, the control variable is the distillate temperature or its composition (measured directly or estimated from temperature measurements) (Aneesh et al., 2016). Nevertheless, Model Predictive Control (MPC) can potentially achieve better control because it uses additional measurements, includes constraints, and considers future references and control actions (Kvernland et al., 2010). Other techniques, such as artificial intelligence-based controllers (Daosud et al., 2016) or coordination auto-tune PI controllers coupled with MPC online optimization (Kumar et al., 2022), could achieve slightly better performance but require much more hardware and time to implement in industrial settings.

Most producers of batch-distilled wine spirits are not using the above techniques to achieve high-quality, more reproducible, and more sustainable products. Possibly, they are not convinced that these techniques are applicable in their challenging environment.

This study integrates rigorous dynamic modeling, disturbance modeling, multiobjective optimization, model predictive control, and Monte Carlo simulations to improve distillation performance and process reproducibility, and reduce cooling water and energy consumption. The variability encountered in actual experimental conditions was modeled to assess its impact on process performance. Then, using multiobjective optimization techniques, we searched for suitable operating trajectories. The control strategies chosen, PI-IMC and MPC, are commonly applied in the process industries because they are simple to tune, typically track varying setpoints, and minimize the impact of measured and unmeasured disturbances. Furthermore, their future implementation and widespread use in the spirits industry will be simplified. Our approach combines the sustainable nature of previous studies but also considers practicality, reproducibility, and adaptability to the variability inherent in real-world batch processes. This approach aligns with the Institute of Chemical Engineers (UK) vision, which underscores the chemical industry's commitment to significantly contribute to a more sustainable world over the next 5 to 10 years. The approach adopted is comprehensively explained in Section 2, followed by the presentation and analysis of the main results in Section 3. The conclusions of this research are presented in Section 4.

2. METHODOLOGY

This section provides a detailed description of the workflow applied to the fruit distillation process. We present a comprehensive model-based workflow that includes the batch-packed column distillation model and the multi-objective optimization methods used to derive optimal operating trajectories. In addition, we describe the controller algorithms implemented to follow these trajectories. The performance of the controller to mitigate the effects of unmeasured disturbances is assessed using Monte Carlo simulations.

2.1. BATCH PACKED-COLUMN DISTILLER SIMULATOR

This subsection describes the distiller simulator used to optimize the operation trajectories and controller design. Firstly, the mathematical model of the distiller is presented. Next, the main performance indices of the distillation process, such as energy and water consumption, are defined. Finally, a disturbance modeling approach represents the experimental variance in a pilot batch distiller at scale.

2.1.1. PROCESS MODEL DESCRIPTION

The pilot distillation system modeled in this study is at the Department of Chemical and Bioprocess Engineering of the Pontificia Universidad Católica de Chile. It has been previously documented by Díaz-Quezada et al. (2015). The dynamic behavior of the main fraction (also known as the heart-cut in spirits distillation) operation is simulated, starting with an initial load of 40 L, 13 %v/v ethanol concentration, and 1.5 g/L a.a. of methanol. The initial settings for the boiler heating power, cooling water flow rate at the partial

condenser, and inlet cooling water temperature were 800 W, 150 mL/min, and 20 ºC, respectively. The control system and disturbance model later defined these inputs. The simulation was run for 8.3 h before ending.

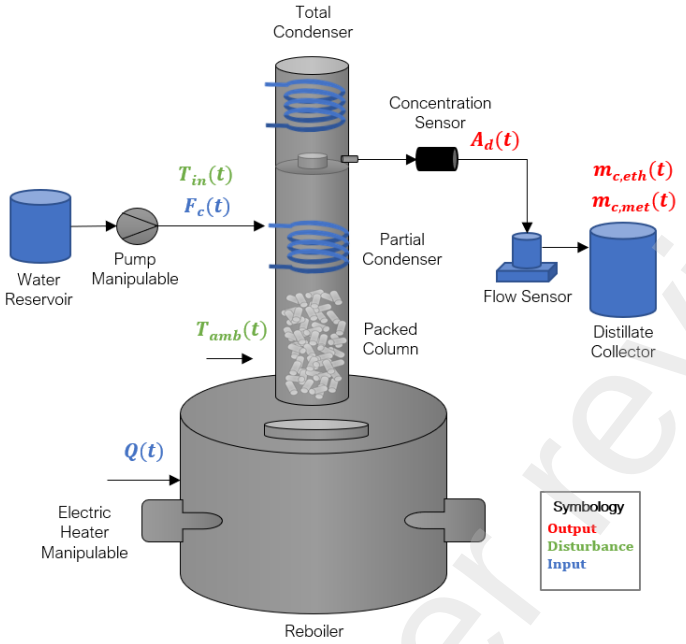

Figure 1. Process diagram of the modeled distillation system.

To model the distillation system accurately (Figure 1), we applied mass and energy balances to each section, including the boiler, rectification column, and partial condenser. The boiler is described by four ordinary differential equations (ODEs) that incorporate three mass balances (total mass, ethanol, and methanol) and an energy balance. In contrast, the packed column requires four partial differential equations (PDEs) to account for the change in temperature and composition with height and time. These PDEs include three mass balances (total mass, ethanol, and methanol) and one energy balance. In addition, two algebraic equations describe the vapor phase equilibrium of methanol and ethanol in the packed column. The partial condenser is considered in a quasi-steady state since its holdup is negligible. Thus, four algebraic equations are used to describe it, including three mass balances and one energy balance. The model also includes a set of constitutive relationships that generate algebraic equations, such as non-ideal vapor/liquid equilibrium, transport properties (diffusion coefficients, viscosities, heat transfer coefficients), physical properties (superficial tensions, densities, heat capacities, vapor and liquid enthalpies, and latent heats), packing hydraulics inside the rectification column, and mass and heat transfer correlations. Please refer to De Lucca et al. (2013) for more detailed information.

To transform the partial differential equations (PDEs) describing the packed column into a more manageable ordinary differential equation (ODE) system, we used the method of lines with finite differences (Chen and Li, 2008; Schiesser and Griffiths, 2009). In this method, the height (z-axis) was discretized into seven elements, resulting in a system that, after some algebra, can be written in the standard semi-explicit notation (Eqs. 1-3). The final differential/algebraic equation system (DAEs) is highly nonlinear. It comprises 31 ODEs (represented by $\boldsymbol{f}$ in Eq. 1), two implicit algebraic equations (represented by $\boldsymbol{h}$ in Eq. 2), and 113 explicit algebraic equations (represented by $\boldsymbol{g}$ in Eq. 3). These equations define the model outputs $\boldsymbol{y}$, such as the temperatures and ethanol concentration in the distillate.

$$\frac{d\boldsymbol{x}}{dt} = \boldsymbol{f}(\boldsymbol{x}(t),\mathbf{w}(t),\boldsymbol{y}(t),\boldsymbol{u}(t),\boldsymbol{p}) \quad (1)$$

$$\mathbf{0} = \boldsymbol{h}(\boldsymbol{x}(t),\mathbf{w}(t),\boldsymbol{y}(t),\boldsymbol{u}(t),\boldsymbol{p}) \quad (2)$$

$$\boldsymbol{y} = \boldsymbol{g}(\boldsymbol{x}(t),\mathbf{w}(t),\boldsymbol{u}(t),\boldsymbol{p}) \quad (3)$$

The resulting system is a nonlinear multivariable input-output (MIMO) system where the implicit equations are solved at each integration step using the algebraic-constraint loop within Matlab/Simulink. For more information about the methodology, model equations, and validation, please refer to our previous work (Diaz-Quezada et al., 2022). In the ideal case (constant inputs without noise), the simulation time is approximately two seconds, using the Matlab ode15s integrator on a desktop computer with 3 GHz (6 cores) and 16 GB of RAM.

2.1.2. DISTILLATION PERFORMANCE INDICES

We selected a set of six performance indices to compare distillation scenarios based on their quality, energy consumption, and water consumption. Each is expressed as a percentage to make the indices' scale more readable.

The first index measures minimum ethanol concentration, which directly impacts distillate quality. Previous work (Balcerek et al., 2017; Luna et al., 2019; Spaho, 2017) has established a critical link whereby lower alcohol content introduces unwanted tail-cut aromas into the distillate, negatively impacting distillate quality:

$$\%Eth.\,min. = \min(A_d(t)), \tag{4}$$

where the variable A_d represents the ethanol concentration in the distillate and is already expressed as a percentage (%v/v).

The second index considers the average ethanol concentration in the collector. This index reflects the bulk quality of the distillate at the end of the distillation process. Higher values are associated with superior distillate quality.

$$\%Eth.\,avg. = A_c(t_{end}), \tag{5}$$

where A_c is the ethanol concentration in the distillate collector; this variable is already in percentage (%v/v).

The third and fourth indices are the mass recovery of the ethanol and methanol in the distillate. High recoveries of ethanol are favorable since they mean high productivity, while in the case of methanol, lower recoveries are desirable because it is a toxic compound. The expressions are respectively:

$$\%Rec.\,Eth. = \frac{m_{c,eth}(t_{end})}{m_{eth}(t_{ini})}100, \tag{6}$$

$$\%Rec.\,Met. = \frac{m_{c,met}(t_{end})}{m_{met}(t_{ini})}100, \tag{7}$$

where $m_{c,eth}$ and $m_{c,met}$ are the ethanol and methanol mass, respectively. These variables are evaluated at the end and initial time to obtain the recovery.

The fifth index is the energy consumed by the boiler during distillation. This index summarizes the total energy footprint of the distillation operation. It provides valuable insight into the efficiency of the process and helps to understand the overall environmental impact of distillation.

$$\%Heat = \frac{\int_0^{t_{end}} Q(t)\,dt}{Q_{max}\ t_{end}}100, \tag{8}$$

Q is the heat power integrated over the distillation time to obtain the total energy. This value is divided by the maximum energy if the entire distillation were to operate at its maximum heating power, Q_{max}.

The sixth and last index is the water consumption in the partial condenser for the reflux in the packed column, which has essentially the same structure as equation (8). This index represents a key aspect of sustainability in the distillation process, especially in northern Chile, where water scarcity is a critical issue.

The efficient use of water in the process ensures the conservation of this valuable resource and contributes to the sustainability of the distillation process.

$$\%Water = \frac{\int_0^{t_{end}} F\,(t)\,dt}{F_{c_{max}}\,t_{end}}\,100, \tag{9}$$

where F_c is the cooling water flowrate, which is integrated over the distillation time to obtain the total water used. This value is divided by the maximum water if the entire distillation were to operate at its maximum cooling flowrate capacity, $F_{c_{max}}$.

2.1.3. DISTURBANCES MODELING

The disturbances modeling task aimed to replicate the experimental variance observed in several distillations, considering parameters (uncertainties) and inputs (disturbances) variability. To accomplish this, we selected the non-manipulable inputs as disturbances, denoted by $\boldsymbol{u_d}$ (inlet coolant water and ambient temperatures). For parameter uncertainties, we chose the three most sensitive model parameters, denoted by $\boldsymbol{p_d}$.

Our approach takes the nominal value of each perturbed variable and then adds a slow time pattern of White Gaussian Noise values over a long period (8 min sample time). This noise model, typically used for disturbance representation (Ramasamy et al., 2019), resulted in a sequence of random step changes with different phases for each disturbance to avoid their superposition, as shown in Eqs. (10) and (11). Additionally, each random disturbance signal started with a different value to generate sequences that differed from each other for the same simulation, as well as between the *m* reproducible batches of distillation simulations.

The signal for the input disturbances was defined by:

$$\boldsymbol{u}_d(t_k) = \boldsymbol{u}_{d,nom} + \boldsymbol{\epsilon_u}(t_k - \boldsymbol{\theta}_{d,u}), \tag{10}$$

here $\boldsymbol{u}_{d,nom}$ is the vector of nominal values for each disturbance input, $[T_{in,nom}\,, T_{amb,nom}]^T$. Furthermore, $\boldsymbol{\epsilon_u}(t_k)$ is the vector signal of random values from an initial condition, with zero mean and a variance matrix obtained from the diagonal with the expected variances of each input $\left[\sigma^2_{T_{in}}, \sigma^2_{T_{amb}}\right]^T$. The delay is included to avoid superposition of the other signals, $\boldsymbol{\theta}_{d,u} = [\theta_{T_{in}}, \theta_{T_{amb}}]^T$.

We followed a similar approach to model the time-varying parameter uncertainties:

$$\boldsymbol{p}_d(t_k) = \boldsymbol{p}_{d,nom} + \boldsymbol{\epsilon_p}(t_k - \boldsymbol{\theta}_{d,p}), \tag{11}$$

where $\boldsymbol{p}_{d,nom}$ is the vector of nominal values for each parameter with uncertainty, $[\phi_{area,nom}\,, UA_{nom}, UA_{c,nom}]^T$. Like input disturbances, the parameter uncertainties are given by the signal of random values, $\boldsymbol{\epsilon_p}(t_k)$, the variance matrix with the diagonal variances, $\left[\sigma^2_{\phi_{area}}, \sigma^2_{UA}, \sigma^2_{UA_c}\right]^T$, and the delay, $\boldsymbol{\theta}_{p,u} = [\theta_{\phi_{area}}, \theta_{UA}, \theta_{UA_c}]^T$.

The parameters for disturbance signals were established by trial and error to capture the temporal ethanol evolution observed in experimental distillations, as detailed in Section 3.1. Hence, Monte Carlo simulations can be applied to asses the performance of the controllers in Section 3.3.

2.2. OPERATION TRAJECTORIES OBTAINED USING MULTIOBJECTIVE OPTIMIZATION

In batch distillation, the performance of the process is influenced by the inputs Q and F, and by the disturbances T_{in} and T_{amb}.

To optimize the process, we focused on finding the best time trajectory for the water-cooling flowrate $F(t)$ within a specified batch time that improves simultaneously more than one distillation performance indices (Section 2.1.2). We aim to define the two most relevant objectives from a sustainable and productive point of view; therefore, this trajectory should minimize water consumption ($\%\,Water$) while maximizing the quality of the distillate ($\%\,Eth.\,avg$). These two objectives conflict due to the nature of the process: the more water used, the higher the ethanol concentration (higher quality). To set up this multiobjective optimization problem, we assumed a nominal scenario with no input disturbances or parameter uncertainties. The coolant flowrate, F,

was discretized into ten elements equally spaced along the distillation process. The first value was fixed at the initial consistent condition for the DAE system, and the remaining nine values were constrained by the maximum pump capacity (500 mL/min) and a minimum flowrate to ensure internal reflux (10 mL/min). The optimization problem was formulated as follows:

$$\min_{F_i} J = [\,\%Water(F_i)\,,\%Eth.\,avg(F_i)\,]^T \quad (12)$$

$$\text{s.t. } F_{min} \le F_i \le F_{max}, \quad i = 1,2,...,9 \quad (13)$$

here, F_i represents the zero-order hold coolant flowrate in the nine elements, and its total was calculated using Eq. (9) to obtain the first objective ($\%Water$). Solving these equations coupled with the batch distiller equation system (Eqs. (1)-(3)) requires significant computational effort. To find the solution for the coolant flowrate trajectory, we used three methods: random search (section 2.2.1), NSGA-II (section 2.2.2) (Deb et al., 2000), and TSEMO (section 2.2.3) (Bradford et al., 2018b), where the last two are genetic algorithms for multiobjective optimization. We applied these MOO algorithms to increase the likelihood of obtaining a diverse and comprehensive set of optimal solutions defining the Pareto set of non-dominated points. These methods differ from scalar methods, such as weighted sum, which makes it difficult to obtain a wide range of solutions during weight tuning (Marler and Arora, 2004). Scalar methods often result in a limited set of solutions. Selecting an optimal solution from the Pareto set requires applying a multi-criteria decision-making (MCMD) technique. The TOPSIS criteria, which provide a balanced trade-off among the objectives (Krishnan et al., 2023), are recommended to achieve the best results. This approach has been successfully applied in similar studies on spirits (Luna et al., 2021). This optimization strategy is summarized in Figure 2.

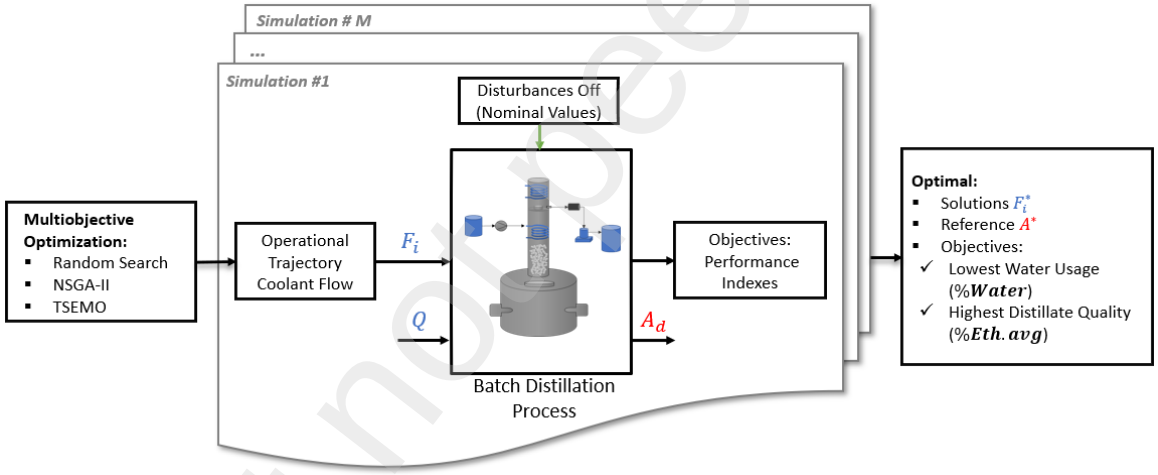

Figure 2. Multiobjective optimization methodology.

2.2.1. RANDOM SEARCH EXPLORATION

The random search method explores the solution space by generating a random combination matrix of samples using the Latin Hypercube method (Castillo, 2007), available through the MATLAB function `lhsdesign`. In this method, we generated 10,000 samples, each defining a different set of the nine columns representing the values for discretized $F(t)$, ranging from 10-500 mL/min.

The aim was to identify the best solutions based on the dominance criterion, where these solutions cannot be improved in $\%Water$ without degrading $\%\,Eth.\,avg$. These solutions, denoted as F_i^*, are also known as non-dominated solutions and belong to the Pareto set. However, due to the random exploratory nature of this method, there is no guarantee of obtaining a detailed "True" Pareto front. Nevertheless, it serves as a good starting point for further optimization.

2.2.2. NSGA-II MULTIOBJECTIVE OPTIMIZATION

NSGA-II is a widely used genetic algorithm for solving multiobjective optimization problems (Yaghoubzadeh-Bavandpour et al., 2022), which incorporates evolutionary features such as selection, crossover, and mutation. Its key attribute is the fast elitist approach that facilitates the discovery of diverse points on the optimal Pareto front. The algorithm was first introduced by Deb et al. (2000).

We solved the MOO problem in MATLAB using the NSGA-II code provided by Lin (2011), with a recommended population size of 600 and 300 generations. We provided the non-dominated solution of coolant flowrate trajectories obtained as the initial guess from the random search method (section 2.2.1). The NSGA-II algorithm produced several trajectories, referred to as NSGA-II non-dominated solutions. These solutions cover a wide range of optimal solutions, allowing us to explore the trade-offs between the two objective functions.

2.2.3. TSEMO MULTIOBJECTIVE OPTIMIZATION

TSEMO is a powerful optimization algorithm that utilizes Thompson sampling and efficient techniques to solve multiobjective optimization problems (Bradford et al., 2018b). The algorithm employs Gaussian process surrogate models, spectral sampling, and genetic algorithms to navigate the objective function space efficiently. Compared to previous genetic algorithms like NSGA-II and ParEGO (Knowles, 2006), this algorithm was found to be competitive in some cases involving expensive to assess objective functions.

To apply this algorithm to our specific problem, we implemented the MATLAB code from the original research paper by Bradford, Schweidtmann, and Felton (2018a). Following the procedure in the code, we defined the data set grid points based on a Latin hypercube matrix with 1350 samples (150 times the number of design variables, 9 in our case) and nine columns. We obtained several trajectories, denominated TSEMO non-dominated solutions. These solutions represented the best trade-offs between conflicting design objectives and helped us make informed decisions about the optimal choices for our problem.

2.3. CONTROL DESING

Controller strategies are critical in achieving effective disturbances rejection and trajectory tracking. The disturbances considered in this study include ambient and input cooling water temperatures, $\boldsymbol{u}_d$, and uncertainties in parameters, $\boldsymbol{p}_d$. To track predefined trajectories, multiobjective optimization algorithms were applied to determine the optimal trajectory, $F_i^*(t)$, which yields the optimal (* symbol) ethanol concentration trajectory, A^*; this trajectory is the set point of the control system.

In this study, two controller strategies, PI-IMC and MPC, were explored. PI-IMC is a commonly used control design strategy in various process industries for its simplicity and effectiveness, though it is limited to manipulating a single process variable. On the other hand, MPC is a more advanced approach that accommodates explicit process constraints and can handle multiple input variables. Although the MPC was designed for systems with multiple inputs and outputs (MIMO), we applied it to control a single output variable (MISO) in our application.

2.3.1. PI-IMC CONTROLLER DESIGN

PI controllers are widely used in control systems due to their easy implementation, low-cost hardware, and minimum instrumentation requirements. In this study, Q was the selected manipulated variable, while the coolant flowrate followed a predefined trajectory, F_i^*. The PI controller aims to reduce the error between the measured ethanol concentration in the distillate, A, and the specified trajectory, A^*, as seen in Figure 3.

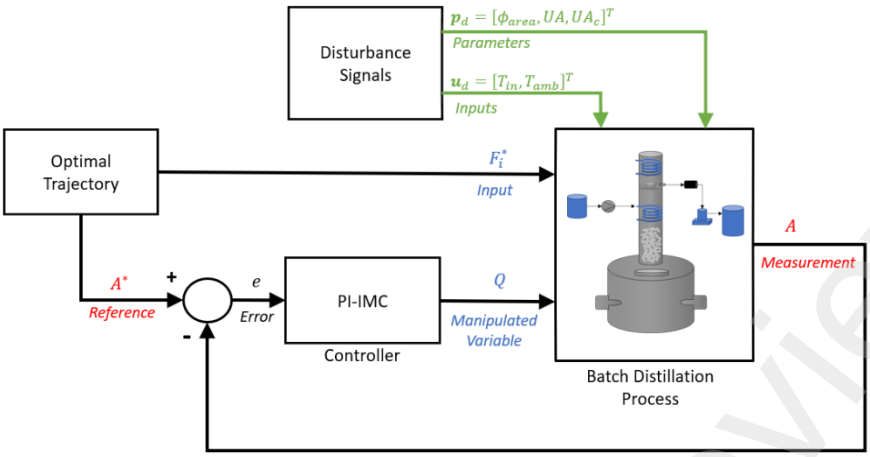

Figure 3. Block diagram of the PI-IMC controlled system.

The control action over the manipulated variable is defined by:

$$Q(t) = K_c\left(1 + \frac{1}{\tau_I}\int_0^t (A^* - A)dt + \tau_D\frac{de}{dt}\right) + Q_0 \qquad (14)$$

The control parameters, K_c and τ_I, were determined using the Internal Model Control (IMC) rules (Manfred Morari and Zafiriou, 1989; Skogestad, 2004), which depend on the model response type. We found that a first-order model plus dead time (FOPDT) with parameters $K_P = -0.0228$ (% v/v)/W, $\tau_P = 42.31$ s, and $\theta_p = 79.82$ s was sufficient to capture the relevant dynamics (see **Appendix 2** for details regarding the system identification procedure).

The control parameter equations are given by:

$$K_c = \frac{1}{K_P}\frac{\tau_P}{\lambda + \theta} \qquad (15)$$

$$\tau_I = \min\{\tau_P, 4(\lambda + \theta)\} \qquad (16)$$

where K_c and τ_I are the controller parameters. The IMC filter constant λ is the tunning parameter; for a stable and robust response, its values should be constrained ($|\tau_P/\lambda| \leq 20$). We started the trial and error tunning procedure with an λ value near the dead time θ, following recommendations by Grimholt and Skogestad (2018).

The controller's overall performance was evaluated based on two typical metrics in control process engineering: the Integral of Absolute Error (IAE), which quantifies the reference tracking accuracy (ideally zero), and the Integral of Absolute Manipulable-Input Variability (IAUV), which quantifies the smoothness of the variable control action effort (which should be minimum). IAE and IAUV require a zero-order hold function to discretize the signals; here, we considered a sample time (Δt) of 8 s. These performance metrics were calculated using the following equations:

$$IAE = \sum |A^* - A| \qquad (17)$$

$$IAUV = \sum \left|\frac{\Delta Q}{\Delta t}\right| \qquad (18)$$

2.3.2. MPC CONTROLLER DESIGN

MPC is a widely used control algorithm in chemical processes such as batch distillations (Kvernland et al., 2010; Meidanshahi et al., 2017; Wilson and Young, 2006) because it can handle multivariable systems, including process and input/output constraints, and could handle some model uncertainties. This controller solves an optimization problem at each time step, where the best control action minimizes the quadratic cost function (J):

$$\min_{(u)} J(k) = \sum_{i=0}^{N_p-1} \left(e^T(k+i)\, w_A\, e(k+i)\right) + \sum_{j=1}^{N_c-1} \left(u^T(k+i)\, w_u\, u(k+i)\right) + \left(\Delta u^T(k+i)\, w_{\Delta u}\, \Delta u(k+i)\right) \tag{19}$$

$$e(k+i) = \frac{1}{A_{max} - A_{min}} \left(A^*(k+i+1|k) - \hat{A}(k+i+1|k)\right) \tag{20}$$

$$u(k+i) = \text{diag}\left(\frac{1}{Q_{max} - Q_{min}}, \frac{1}{F_{max} - F_{min}}\right)\left([Q,F]_{target}(k+i|k) - [Q,F](k+i+1|k)\right) \tag{21}$$

$$\Delta u(k+i) = u(k+i) - u(k+i-1) \tag{22}$$

Here, the controlled variable is the ethanol concentration prediction, $\hat{A}_d$, and the ethanol reference trajectory is A^*. The control action considers two manipulated variables, Q and F. All variables are evaluated at the k discrete time considering a sample time (Δt) of 8 s. The additional weighting parameters, namely w_A, w_u, and $w_{\Delta u}$, are defined and discussed in the results section.

Moreover, the controller has additional features, such as future reference tracking of the ethanol concentration trajectory over the prediction horizon (N_p). Anticipated reference tracking allows the controller to prevent the impact of significant changes with its look-ahead characteristic and compute the next control action accordingly over the control horizon (N_c). Additionally, disturbed temperature measurements enable the MPC to compensate for expected dynamic disturbances, reducing their impact on the distillation process. Like the PI-IMC strategy, the optimal trajectory, F_i^*, is predefined. The resulting control strategy diagram is depicted in Figure 4 below.

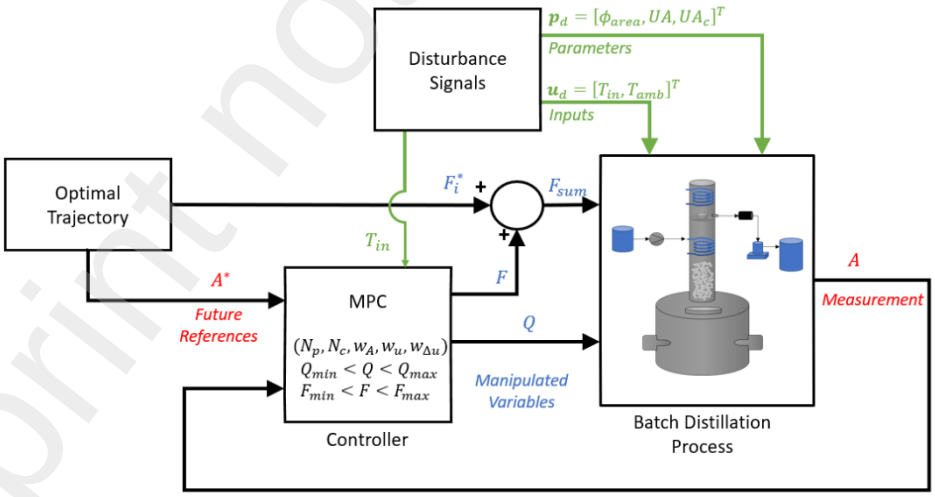

Figure 4. Block Diagram of MPC Controller.

This controller was implemented in MATLAB/Simulink using the standard "MPC Controller" block. Here, an object is created with the function `mpc`, where all the MPC parameters are defined.

In this case, the IAUV index is a column vector since the discretized control action comprises two manipulated variables:

$$IAUV = \left[\sum \left| \frac{\Delta Q}{\Delta t} \right| , \sum \left| \frac{\Delta F}{\Delta t} \right| \right]^T \quad (23)$$

3. Results and Discussion

In this section, we assess the appropriate disturbance model that replicates the experimental distillations. We also analyze the Pareto front obtained with three multiobjective optimization algorithms. Furthermore, we evaluate the effectiveness of two controllers in tracking two optimal operating trajectories of the distillation process under the influence of disturbances.

3.1. Disturbance Modelling

Drawing from the experimental data presented by Díaz et al. (2015), we aim to identify a configuration of disturbances for parameters and inputs that adequately replicate the variability of the ethanol concentration evolution observed in 15 experimental distillations.

To simulate the disturbances, we explored various variance values and strategically introduced phase delays to ensure that the disturbances were well-spaced and evenly distributed over time. This careful timing avoids simultaneous changes from multiple disturbances, creating a challenging and realistic scenario for the disturbance model. This method enabled modeling time-varying disturbances as random noise signals with an 8-minute sampling interval. Fifty distinct random signals (disturbance patterns) were generated to capture a broad array of possible simulated distillations (for further details, please refer to **Appendix 3**). The following table details the defined parameters:

Table 1. Disturbance configuration.

Disturbance	Nominal Value	Std. Deviation (σ)	Phase Delay (θ)
T_{in}	293 K	8 K	0.1 min
T_{amb}	303 K	8 K	0.5 min
ϕ_{area}	0.800 (-)	0.002 (-)	1.5 min
UA	0.358 W/m^{2}K	0.007 W/m^{2}K	2.0 min
UA_c	7.0 W/m^{2}K	1.2 W/m^{2}K	2.5 min

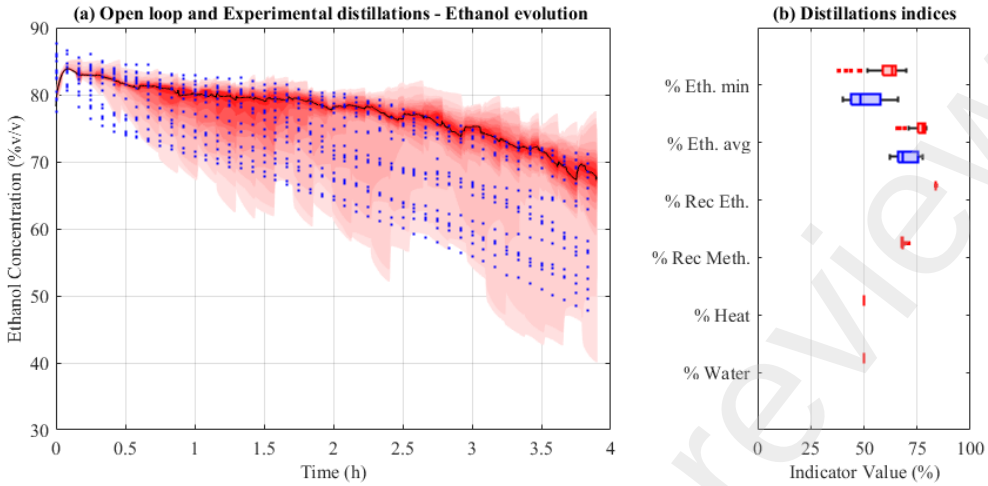

Figure 5. Simulated distillations and experimental distillations. Left graph **(a):** simulations at 95 % confidence interval (**red shades**); median simulation (**black line -**); experimental values (**blue dots ●**). Right graph **(b):** Performance indices obtained using experimental data (**blue boxplots ◫**) and simulations (**red boxplots ◫**).

In Figure 5(a), the simulation results generated with the defined disturbances outlined in Table 1 are compared with the experimental data. It can be observed that the trend and variability of the evolution of ethanol concentration in the open loop (uncontrolled) distillations (red shadows) and the experimental distillations (blue dots) are similar. The intensity of the red shading represents the frequency of ethanol concentration values, with darker shades indicating areas of higher occurrence. Additionally, in the boxplot (Figure 5(b)), the variabilities of the performance indices are shown; these were calculated from the open loop distillations (in red). The variabilities associated with ethanol are quite similar to the experimental ones (in blue). Hence, the distiller and associated disturbance models adequately represent the experimental distillations.

The significance of process variability in distillation has been acknowledged. However, Luna et al. (2021) and Parhi et al. (2019) have faced this issue differently. Thus, further exploration is necessary to develop solutions that effectively encompass the time-varying nature of these processes. Diwekar (2005) and Fu & Diwekar (2004) contributed significantly by utilizing variance Fisher information and probabilistic uncertainty analysis. However, these techniques do not consider the inherent temporal variability in batch distillation processes. Our research contributes to this field by offering simulation and experimental distillations incorporating time-varying disturbances. This approach enhances the result's realism and fills the gaps left by the mentioned studies.

3.2. Operation Trajectories

The second task involved finding an operational trajectory for the coolant flowrate policy while keeping the heating power constant at 50 % duty. It is important to note that the time-varying disturbances were disabled while obtaining these trajectories.

Given the objectives of minimizing cooling water consumption and maximizing the average ethanol concentration as a trade-off case, the optimal solutions are represented on a Pareto front. This front illustrates the compromise between conflicting objectives, where any improvement in one objective would lead to a concession in the other. The results of the three proposed methodologies for this multiobjective optimization problem are plotted on the Pareto front in the following figure:

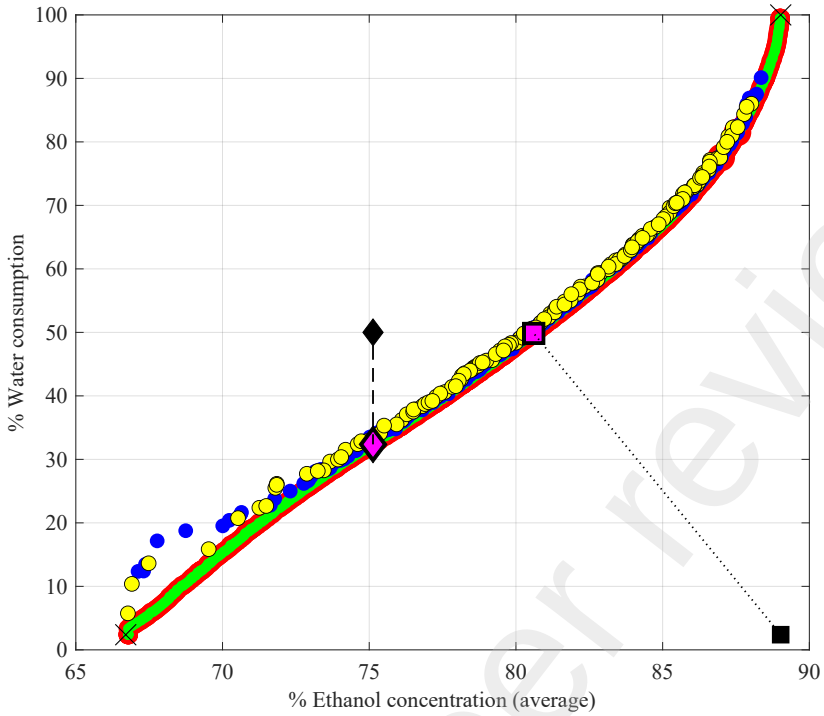

Figure 6. Pareto Front. Non-dominated solutions from Random Search (blue dots ●); NSGA solutions (green dots ●); TSEMO solutions (yellow dots ●); Global Non-dominated solutions (red edge ○); Feasible limits (black cross ✕); Trajectory #1 (pink diamond ◆), Trajectory #2 (pink square ■); Mean point, at the centroid of feasible area, (black diamond ◆); Utopian point (black square ■); Projection distance from Mean point to Trajectory #1 (black segmented line --); and Closest distance from Utopian point to Trajectory #2 (black dotted line **:**).

Figure 6 showcases the outcomes of three distinct multiobjective optimization algorithms: Random Search, NSGA-II, and TSEMO. The NSGA-II algorithm has yielded a continuous and densely populated Pareto front, evident from the green dots bordered by a red edge. The Random Search and TSEMO methods, represented by blue and yellow dots, respectively, largely intersect with NSGA-II's results in the front's central region, achieving comparable outcomes. However, they do not surpass the performance of NSGA-II. Notably, performance diverges near the boundaries of the solution space; Random Search and TSEMO appear to falter, not approaching the Pareto front as closely as NSGA-II or failing to find optimal solutions, mostly at high ethanol concentrations.

Implementing the random search method was straightforward compared to the other two methods. Tuning the NSGA-II and TSEMO required additional effort, involving extensive testing of various functions and parameters. We allocated a similar computation time frame of approximately 4-5 hours for each method. Due to the complex nature of our model, which includes a large set of differential equations and a few implicit algebraic equations, parallel computing was essential to enhance running-time efficiency. This model was particularly challenging for TSEMO; hence, we had to modify the original code to allow parallel processing. In contrast, while not aligning perfectly with the Pareto front, the random search proved a quick and uncomplicated approach for deriving suboptimal yet high-quality solutions near the Pareto front. NSGA-II, however, excelled by producing a more expansive and densely populated Pareto front, in alignment with the results from other studies in multiobjective optimization, highlighting its ability to generate well-distributed fronts across multiple objectives (Parhi et al., 2019; Sarkar et al., 2006; Tarafder et al., 2007).

From the Pareto front, two solutions were selected for further analysis. As a reference, we took the "mean point" of the Random Search (black diamond) as heuristical selection, corresponding to the centroid of the feasible area, characterized by 50 % water consumption and 75.1 % ethanol of the distillate. When this point

was projected onto the Pareto front, a remarkable solution emerged: it reflected the same ethanol quality but had an impressive 35 % reduction in water consumption (represented by a pink diamond at 75.1 % ethanol concentration and 32.7 % water consumption). We named this solution Trajectory #1.

Our second choice from the Pareto front was the closest to the utopian point (pink square; 49.2 % water consumption and 80.4 % ethanol concentration). Based on multiobjective optimization principles, this choice aligns with the TOPSIS methodology (Krishnan et al., 2023; Luna et al., 2021); we named this solution Trajectory #2. Notably, this trajectory highlights the optimal balance between objectives. Compared to the mean point, it reduces water consumption by 4 % while increasing ethanol quality significantly (+7 %). It's important to note that these results were obtained without considering disturbances.

Thus, these two trajectories were simulated 50 times in an open loop (uncontrolled) to assess the impact of the disturbances in the variability of the distillation process, as is shown in Figs. 7 and 8; these results are the baseline for the controller implementation for disturbances rejection.

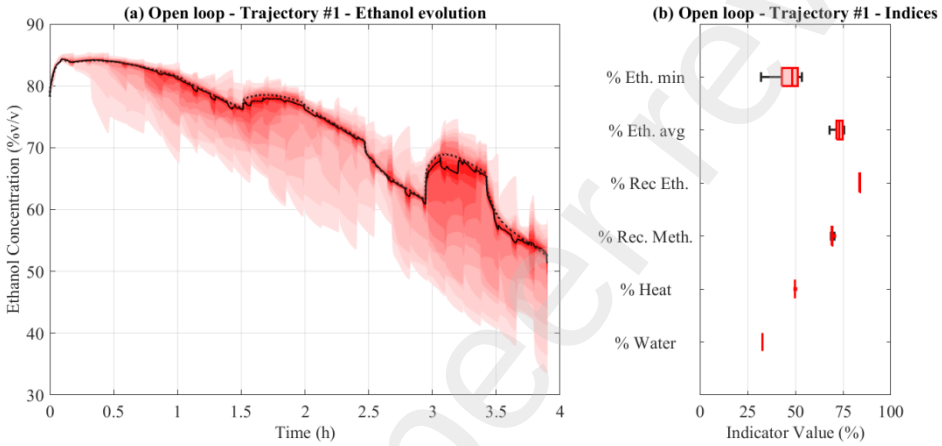

Figure 7. Open loop simulation distillations following the coolant flowrate policy Trajectory #1: "Projected Mean Point." Left graph of ethanol concentration evolution **(a):** results at 95 % confidence interval (**red shades**); the median time-values (**black line -**); without disturbances (**dotted line** ⋯). Right graph **(b):** Performance indicators obtained (**red boxplots**).

In Figure 7(a), the open loop distillations operating under Trajectory #1 are shown. The ethanol concentration response is characterized by abrupt changes between high and low values and the typical overall decrease observed in batch spirit distillations. The red-shaded area, covering the 95 % confidence interval of the simulations (same as before; darker intensity means highly frequent values), illustrates the large variability caused by the modeled disturbances. Additionally, it can be seen that the continuous black line, representing the median of the simulated distillations, deviates significantly from the optimal trajectory (dashed line) at the end of the process. Moreover, according to **Figure** 7(b), the process variability affected the minimum and average ethanol concentrations the most. Consequently, the process variability due to open loop operation under standard disturbances causes significant degradation of the spirit quality.

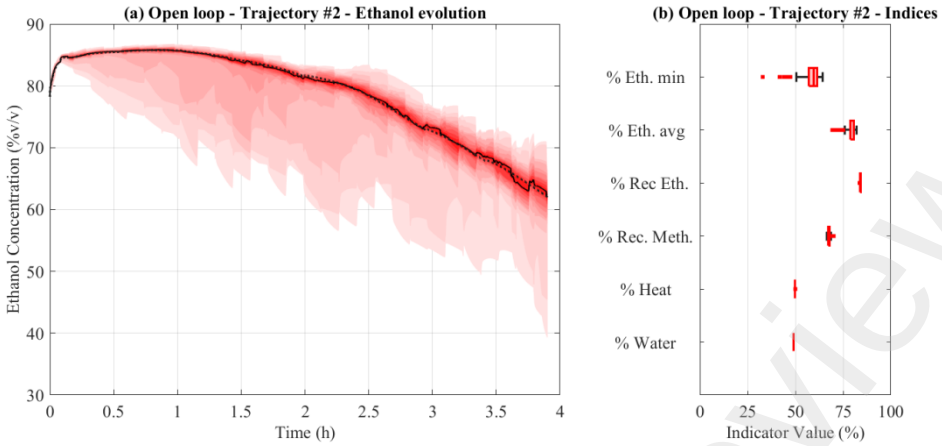

Figure 8. Open loop distillations following the coolant flow policy Trajectory #2: "Minimal distance to Utopic Point." Left graph of ethanol concentration evolution **(a):** results at 95 % confidence interval (**red shades**); the median time-values (**black line -**); without disturbances (**dotted line** ⋯). Right graph **(b):** Performance indicators obtained (**red boxplots** ◫).

Figure 8(a) displays the distillation following Trajectory #2, which produces a much smoother ethanol concentration response in addition to the natural decline in concentration (the black median line). The variability of the response due to disturbances is similar to that shown in Figure 7(a), as illustrated by red-shaded areas of similar width. Moreover, Figure 8(b) reveals that the indices most sensitive to variability are the minimum (% Eth. min) and average ethanol concentrations (% Eth. avg).

This study demonstrates the application of multiobjective optimization algorithms to achieve sustainable distillation operations, as Aneesh et al., (2016) outlined. It also addresses the sustainability concerns that Becker et al. (2020) raised in the spirits sector.

3.3. Control Performance

In the following sections, we compare PI-IMC and MPC controllers and evaluate their performance using metrics such as IAE and IAUV while tracking Trajectories #1 and #2. We also examine the extent of error and variability these controllers introduce regarding ethanol concentration in the distillate and other performance indices.

3.3.1. PI-IMC

Implementing this controller within our simulator was straightforward, using the standard Simulink block for PID control. Later, searching for the IMC filter constant was necessary for setup and tuning. We fine-tuned the controller and determined that the optimal IMC constant filter was $\lambda = 65.65$ s. This value provided a balanced trade-off between the IAE and the IAUV. For details regarding the PI-IMC tuning procedure, please refer to **Appendix 4**.

In **Figure 9** and **Figure 10**, the results of the PI-IMC controller are shown.

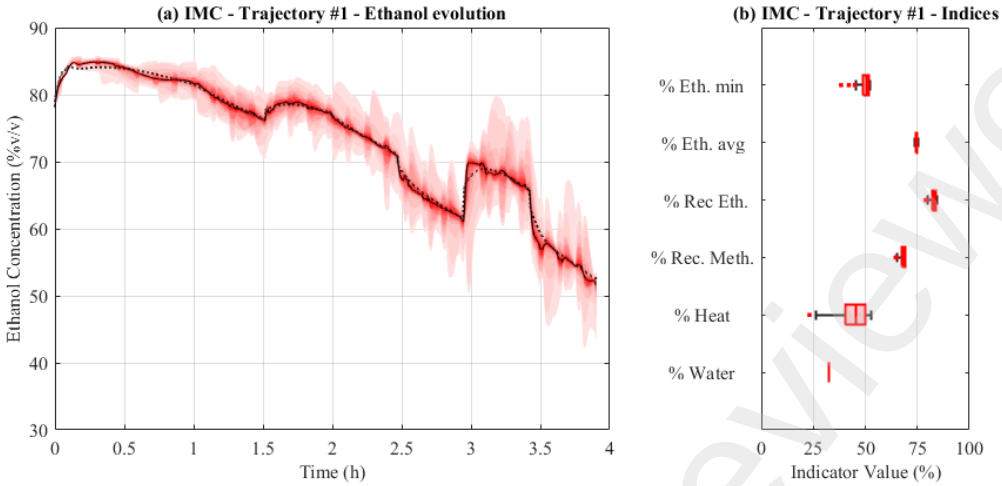

Figure 9. PI-IMC Results following the ethanol concentration reference from Trajectory #1: "Projected Mean Point." Left graph of ethanol concentration evolution **(a):** results at 95 % confidence interval (**red shades**); the median time-values (**black line -**); Setpoint values (**dotted line** ⋯). Right graph **(b):** Performance indicators obtained (**red boxplots** ◫).

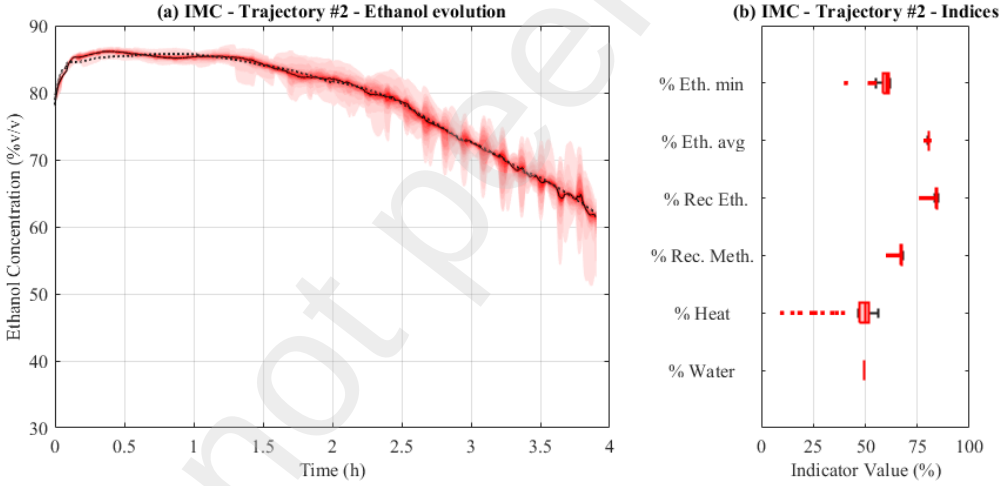

Figure 10. PI-IMC Results following the ethanol concentration reference from Trajectory #2: "Minimal distance to Utopic Point." Left graph of ethanol concentration evolution **(a):** results at 95 % confidence interval (**red shades**); the median time-values (**black line -**); Setpoint values (**dotted line** ⋯). Right graph **(b):** Performance indicators obtained (**red boxplots** ◫).

In summary, the controller effectively reduced the impact of the simulated disturbances on the evolution of the ethanol concentration and the minimum and average ethanol concentrations in both trajectories compared with the corresponding open-loop simulations. Trajectory #1 was more challenging to track due to its abrupt setpoint changes, resulting in larger control errors. In contrast, the controller performed better when tracking Trajectory #2. In both cases, the median of the simulations closely tracked the set point throughout the distillation process, resulting in only small deviations. Notably, the PI-IMC control resulted in significantly smaller deviations than the open-loop cases. Comparatively, Trajectory #2 showed the smallest deviations; however, an oscillatory response was observed, which may be related to the sudden changes in the modeled disturbances. Nevertheless, the controller could not avoid variations in the recovered ethanol and methanol. A more detailed comparison is presented in Section 3.4, considering process and control performance indices.

3.3.2. MODEL PREDICTIVE CONTROLLER

This second controller was implemented using the standard Simulink MPC block. Given the large number of tuning parameters, the controller configuration was more difficult than the PI-IMC, in addition to preparing the ethanol concentration setpoint vectors for the look-ahead mechanism. The MPC tunning parameters were obtained by optimal trade-off among IAE and IAUV's indices during exploration based on Latin Hypercube sampling. Given the nonlinear nature of the process model, these indices are sensitive to the control parameters. Nonlinear control algorithms can achieve even more robust performance, but these are more difficult to implement. The MPC parameters applied were: prediction horizon $N_p = 100$ (larger value due to the long dead time θ_p), control horizon $N_c = 3$, prediction weight $w_A = 0.229$, weight of the control action move $w_{\Delta u} = [0.045, 0.009]$, and weight for target deviation in the control action $w_u = [0.279, 0.057]$. For more information on the MPC tuning procedure, please refer to **Appendix 5**.

The results of the MPC controller are shown in **Figure 11** and **Figure 12**.

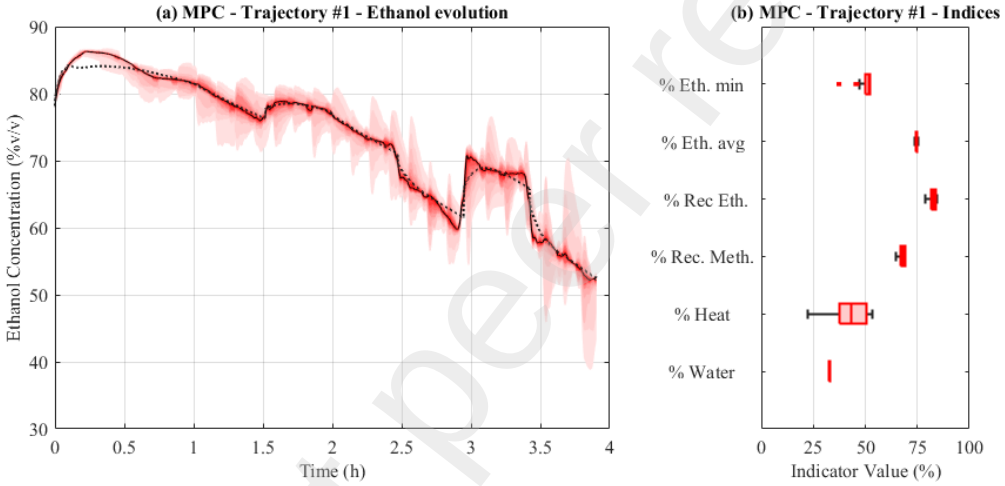

Figure 11. MPC results following the ethanol concentration reference from Trajectory #1: "Projected Mean Point." Left graph of ethanol concentration evolution **(a):** results at 95 % confidence interval (**red shades**); the median time-values (**black line -**); Setpoint values (**dotted line** ⋯). Right graph **(b):** Performance indicators obtained (**red boxplots** ◫).

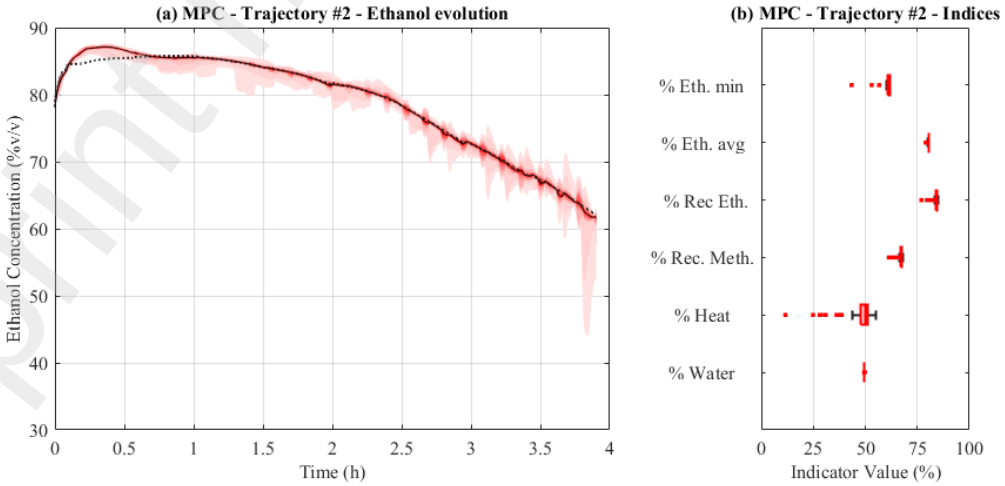

Figure 12. MPC Results following the ethanol concentration reference from Trajectory #2: "Minimal distance to Utopic Point." Left graph of ethanol concentration evolution **(a):** results at 95 % confidence interval

(**red shades**); the median time-values (**black line -**); without disturbances (**dotted line ⋯**). Right graph **(b):** Performance indicators obtained (**red boxplots ◫**).

This study has shown that Model Predictive Control (MPC) is effective in dealing with the complex nature of batch distillation since it can adapt to difficult situations and reduce the effects of disturbances on ethanol concentration. According to Kvernland et al. (2010), Wilson and Young (2006), and Nolasco et al. (2021), MPC is good at handling unexpected changes and tracking variable set points because it can predict future events and deal with multiple constraints simultaneously, which was confirmed by our simulations. MPC was able to significantly reduce the variability in the performance of the distillation process compared to open-loop operation.

At the beginning of the distillation process, it was difficult for MPC to maintain the desired ethanol concentration levels as closely as the Proportional-Integral-Internal Model Control (PI-IMC) system for the first half hour. However, MPC performed very well after this initial period, with only small deviations from the set point.

MPC's ability to "look ahead" and anticipate future changes gives it an advantage in handling sudden changes, as seen in Trajectory #1. This system knows the set point variations in advance, predicts the impact of these variations on the process dynamics, and adjusts the control effort accordingly. In our study, MPC used two variables that could be manipulated simultaneously, giving it greater flexibility and control power to face strong disturbances. In contrast, PI-IMC struggles with nonlinear changes and rapidly changing set points. However, it is simpler, less expensive to implement in an industrial setting, and easier to tune because it has only one tuning parameter. PI-IMC works well in many situations, such as with Trajectory #2. Zou et al. (2017) found that smooth disturbances and set point changes may explain why PI control performance is not severely affected by the nonlinear nature of the process. A typical method used in continuous distillation to smooth process transitions after sudden set point changes under PI control considers a first-order filter applied to the set point function.

In summary, this study shows that both MPC and PI-IMC have strengths in addressing the challenges of batch distillation in packed columns. MPC offers better adaptability and performance, while PI-IMC is simpler and more cost-effective. Therefore, we show the industry that process control techniques can significantly improve the consistency and sustainability of batch distillation processes for spirits.

3.4. Overall Results

The following figure and table summarize the performance indices obtained,

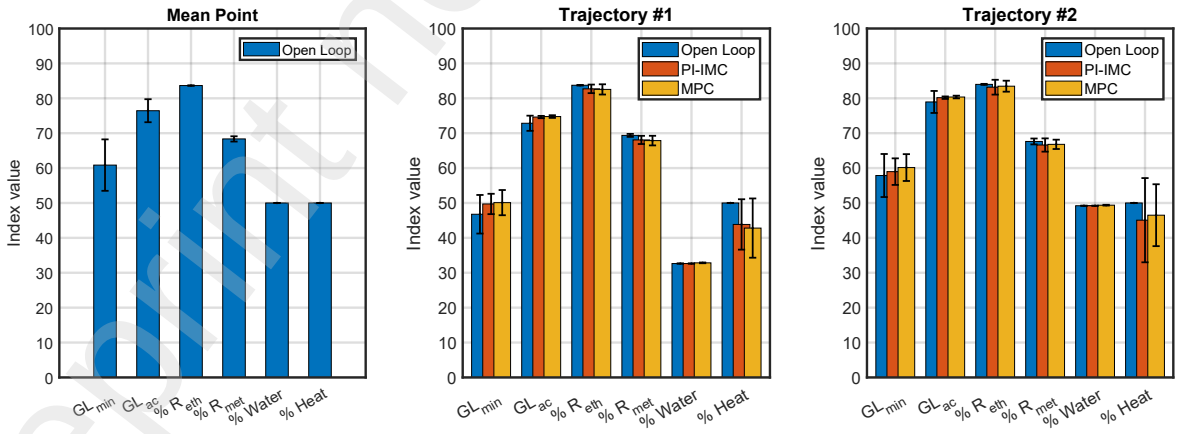

Figure 13. Distillation performance indices comparison. Open loop (blue bar), PI-IMC (red bar), and MPC (orange bar). The left graph is for mean point distillations, the center is for Trajectory #1, and the right is for Trajectory #2.

Table 2. Overall Performance of Open-loop and Closed-loop Distillations (mean values ± one standard deviation).

		Non-optimal policy	Optimal operation policy	
Controller	**Index**	**Mean Point**	**Trajectory #1**	**Trajectory #2**
Open loop (Without controller)	*% Eth. min.*	60.9 ± 7.4	46.8 ± 5.5	57.9 ± 6.2
	% Eth. avg.	76.4 ± 3.3	72.9 ± 2.2	79.0 ± 3.2
	% Rec. Eth.	83.65 ± 0.06	83.74 ± 0.09	83.99 ± 0.15
	% Rec. Meth.	68.36 ± 0.75	69.37 ± 0.42	67.63 ± 0.84
	% Heat	50	50	50
	% Water	50.0	32.6	49.2
	IAE	-	4.1 ± 3.4	2.6 ± 3.6
PI-IMC	*% Eth. min.*	-	49.7 ± 2.9	59.0 ± 3.8
	% Eth. avg.	-	74.63 ± 0.33	80.18 ± 0.36
	% Rec. Eth.	-	82.7 ± 1.2	83.9 ± 2.1
	% Rec. Meth.	-	68.0 ± 1.2	66.6 ± 1.9
	% Heat	-	43.9 ± 7.2	45.1 ± 12.1
	% Water	-	32.6	49.2
	IAE	-	2.0 ± 1.4	0.63 ± 0.45
	$IAUV_Q$	-	0.67 ± 0.44	0.20 ± 0.14
MPC	*% Eth. min.*	-	50.1 ± 3.6	60.2 ± 3.9
	% Eth. avg.	-	74.77 ± 0.38	80.37 ± 0.39
	% Rec. Eth.	-	82.6 ± 1.5	83.5 ± 1.6
	% Rec. Meth.	-	67.9 ± 1.4	66.8 ± 1.3
	% Heat	-	42.8 ± 8.5	46.5 ± 8.9
	% Water	-	32.84 ± 0.11	49.37 ± 0.11
	IAE	-	1.74 ± 0.89	0.49 ± 0.37
	$IAUV_Q$	-	0.17 ± 0.10	0.03 ± 0.02
	$IAUV_F$	-	0.0020 ± 0.0012	0.0004 ± 0.0003

Table 2 and **Figure 13** comprehensively compare distillation performance indices for the open loop, PI-IMC, and MPC controllers.

Significant differences were observed when comparing the performance of the disturbed Mean Point distillations with the disturbed open-loop optimum distillations. When we applied Trajectory #1, water consumption was reduced by up to 35 % but at the expense of distillate quality, which was reduced by 4.5 %. Additionally, the minimum ethanol concentration was lower than the Mean Point distillation. Trajectory #2 performed better than the Mean Point distillation, with a 3.4 % higher ethanol concentration and 1.6 % lower water consumption. Nevertheless, these improvements were about half of what was expected due to the negative impact of the disturbances. It is worth noticing that the Mean Point distillations performed better than the optimum trajectories in terms of minimum ethanol. Consequently, this index could be included in the MOO formulation as an additional objective to find even better trajectories. Since the ethanol and methanol recoveries showed marginal differences among the distillation policies evaluated, their inclusion in the MOO problem would not lead to significantly better trajectories.

Both controllers, PI-IMC and MPC, yielded significantly reduced mean and deviations of the *IAE* index for the optimal trajectories. Moreover, MPC achieved smaller mean and standard deviations of *IAE* in both optimum trajectories than PI-IMC. Additionally, MPC showed much smoother control actions than PI-IMC, as evidenced by the *IAUV* values. Both controllers achieved considerably smaller *IAE* and *IAUV* values with the smooth Trajectory #2. Therefore, applying smooth optimal trajectories in real distillations is recommended as they ensure the production of consistent spirits by minimizing the effect of unpredictable disturbances.

Even though PI-IMC and MPC did not increase the average ethanol significantly and only moderately increased the minimum ethanol (4 %), they remarkably increased distillation reproducibility, reducing close to 10 times the standard deviations of the average ethanol. Considering sustainability, both controllers showed promising results compared to the open-loop scenario. They can enhance ethanol concentrations while reducing up to 14.4 % of the heating power. This performance aligns seamlessly with our ambition to optimize resource usage. Process control is an important step toward a more sustainable operation in terms of resource use, efficiency, and process stability.

4. CONCLUSIONS

Our research significantly advances sustainable distillation practices, specifically tailored to address the critical issues of resource efficiency in the spirit production industry. Through a workflow that integrates rigorous process modeling, disturbance modeling, multiobjective optimization, model predictive control, and Monte Carlo simulations, we achieved a notable reduction in resource consumption—35% in water and 14.4% in energy—while maintaining high distillate quality. The MPC controller demonstrated superior performance in challenging distillation scenarios, providing a compelling case for its wider adoption. The effective integration of these tools reduced the inherent process variability in distillation and controller performance indices by approximately 50 %. Beyond spirits production, the implications of our research extend to other batch distillation industries, where these strategies offer promising avenues for resource optimization and process stabilization. This study provides important insights and identifies areas for further research, such as scalability for industrial applications, additional optimization strategies with new algorithms or objectives selection, and comprehensive, robust controllers with adaptive mechanisms to overcome potential parameter uncertainties or modeling mismatch. Our findings suggest potential avenues for improving sustainability within the spirits industry. Nevertheless, the methodology used in this study can be applied to any other batch process in the pharmaceutical, beer&wine, and food processing industries, which require enhanced quality and reproducibility while considering sustainable operation.

NOMENCLATURE

Variable	Definition
A_d	Ethanol concentration in the distillate (%v/v)
m_{eth}	Methanol mass (kg)
m_{met}	Ethanol mass (k)
T_{in}	Cooling temperature (K)
F_c	Cooling flowrate (mL/min)
T_{amb}	Ambient temperature (K)
Q	Heating power (W)
$\boldsymbol{u_d}$	Non-manipulable inputs as disturbances vector
$\boldsymbol{p_d}$	Parameter under uncertainties vector
e	Error signal between reference and measurement
K_c	Proportional gain of PID controller
τ_I	Integrative time of PID controller
τ_D	Derivative time of PID controller
K_P	Process gain
τ_P	Time constant first order
θ	Dead time
IAE	Integral of Absolute Error
$IAUV$	Integral of Absolute Manipulable-Input Variability
Δt	Sample time
J	Cost function for minimization

w_A	MPC weight for error
w_u	MPC weight for manipulable input
$w_{\Delta u}$	MPC weight for manipulable input variation
N_p	Prediction horizon
N_c	Control horizon
MOO	Multiobjective optimization
MPC	Model Predictive Control
PI-IMC	Proportional Integral/Internal Model Control

REFERENCES

Agosin, E., Belancic, A., Ibacache, A., Baumes, R., Bordeu, E., Crawford, A., Bayonove, C., 2000. Aromatic potential of certain Muscat grape varieties important for Pisco production in Chile. Am. J. Enol. Vitic. 51, 404–408.

Aneesh, V., Antony, R., Paramasivan, G., Selvaraju, N., 2016. Distillation technology and need of simultaneous design and control: A review. Chem. Eng. Process. Process Intensif. 104, 219–242. https://doi.org/10.1016/j.cep.2016.03.016

Arrieta-Garay, Y., Blanco, P., López-Vázquez, C., Rodríguez-Bencomo, J.J., Pérez-Correa, J.R., López, F., Orriols, I., 2014. Effects of distillation system and yeast strain on the aroma profile of Albariño (Vitis vinifera L.) grape pomace spirits. J. Agric. Food Chem. 62, 10552–10560. https://doi.org/10.1021/jf502919n

Balanuta, A., Covaci, E., Sclifos, A., 2021. The influence of distillation methos on the flavor profile and quality indices of wine brandies. J. Eng. Sci. XXVIII, 173–184. https://doi.org/10.52326/jes.utm.2021.28(2).15

Balcerek, M., Pielech-Przybylska, K., Patelski, P., Dziekońska-Kubczak, U., Strąk, E., 2017. The effect of distillation conditions and alcohol content in 'heart' fractions on the concentration of aroma volatiles and undesirable compounds in plum brandies. J. Inst. Brew. 123, 452–463. https://doi.org/10.1002/jib.441

Barbosa, F.S., Scavarda, A.J., Sellitto, M.A., Lopes Marques, D.I., 2018. Sustainability in the winemaking industry: An analysis of Southern Brazilian companies based on a literature review. J. Clean. Prod. 192, 80–87. https://doi.org/10.1016/j.jclepro.2018.04.253

Becker, S., Bouzdine-Chameeva, T., Jaegler, A., 2020. The carbon neutrality principle: A case study in the French spirits sector. J. Clean. Prod. 274, 122739. https://doi.org/10.1016/j.jclepro.2020.122739

Bradford, E., Schweidtmann, A., Felton, K., 2018a. Thompson sampling efficient multiobjective optimization [WWW Document]. GitHub Repos. URL https://github.com/Eric-Bradford/TS-EMO (accessed 1.30.24).

Bradford, E., Schweidtmann, A.M., Lapkin, A., 2018b. Efficient multiobjective optimization employing Gaussian processes, spectral sampling and a genetic algorithm. J. Glob. Optim. 71, 407–438. https://doi.org/10.1007/s10898-018-0609-2

Carvallo, J., Labbe, M., Pérez-Correa, J.R., Zaror, C., Wisniak, J., 2011. Modelling methanol recovery in wine distillation stills with packing columns. Food Control 22, 1322–1332. https://doi.org/10.1016/j.foodcont.2011.02.007

Castillo, E. Del, 2007. Process Optimization, International Series in Operations Research & Management Science. Springer US, Boston, US. https://doi.org/10.1007/978-0-387-71435-6

Chen, Y.-T., Li, J., 2008. Computational Partial Differential Equations Using MATLAB. CRC Press, Florida, US.

Daosud, W., Jariyaboon, K., Kittisupakorn, P., Hussain, M.A., 2016. Neural network based model predictive control of batch extractive distillation process for improving purity of acetone. Eng. J. 20, 47–59. https://doi.org/10.4186/ej.2016.20.1.47

646 De Lucca, F., Munizaga-Miranda, R., Jopia-Castillo, D., Gelmi, C.A., Pérez-Correa, J.R., 2013. Operation
647 strategies to minimize methanol recovery in batch distillation of hydroalcoholic mixtures. Int. J. Food
648 Eng. 9, 259–265. https://doi.org/10.1515/ijfe-2013-0031

649 Deb, K., Agrawal, S., Pratap, A., Meyarivan, T., 2000. A Fast Elitist Non-dominated Sorting Genetic Algorithm
650 for Multi-objective Optimization: NSGA-II, in: CEUR Workshop Proceedings. pp. 849–858.
651 https://doi.org/10.1007/3-540-45356-3_83

652 Díaz-Quezada, S., Pérez-Correa, J., Fernández-Fernández, M., 2015. Automatic System Distillation for Wine
653 Fruit. IEEE Lat. Am. Trans. 13, 1882–1887. https://doi.org/10.1109/TLA.2015.7164212

654 Diaz-Quezada, S., Wilson, D.I., Perez-Correa, J.R., 2022. Modeling and Simulation of a Packed Column Batch
655 Still for Fruit Wine Distillations. IEEE Access 10, 1–1. https://doi.org/10.1109/ACCESS.2022.3197604

656 Diwekar, Amekudzi-Kennedy, A., Bakshi, B., Baumgartner, R., Boumans, R., Burger, P., Cabezas, H., Egler,
657 M., Farley, J., Fath, B., Gleason, T., Huang, Y., Karunanithi, A., Khanna, V., Mangan, A., Mayer, A.L.,
658 Mukherjee, R., Mullally, G., Rico-Ramirez, V., Shonnard, D., Svanström, M., Theis, T., 2021. A
659 perspective on the role of uncertainty in sustainability science and engineering. Resour. Conserv. Recycl.
660 164, 105140. https://doi.org/10.1016/j.resconrec.2020.105140

661 Diwekar, U., 2005. Green process design, industrial ecology, and sustainability: A systems analysis perspective.
662 Resour. Conserv. Recycl. 44, 215–235. https://doi.org/10.1016/j.resconrec.2005.01.007

663 Diwekar, U.M., 2003. Greener by Design. Environ. Sci. Technol. 37, 5432–5444.
664 https://doi.org/10.1021/es0344617

665 Douady, A., Puentes, C., Awad, P., Esteban-Decloux, M., 2019. Batch distillation of spirits: experimental study
666 and simulation of the behaviour of volatile aroma compounds. J. Inst. Brew. 125, 268–283.
667 https://doi.org/10.1002/jib.560

668 Fu, Y., Diwekar, U.M., 2004. An efficient sampling approach to multiobjective optimization. Ann. Oper. Res.
669 132, 109–134. https://doi.org/10.1023/B:ANOR.0000045279.46948.dd

670 García-Llobodanin, L., Roca, J., López, J.R., Pérez-Correa, J.R., López, F., 2011. The lack of reproducibility
671 of different distillation techniques and its impact on pear spirit composition. Int. J. Food Sci. Technol. 46,
672 1956–1963. https://doi.org/10.1111/j.1365-2621.2011.02707.x

673 Grimholt, C., Skogestad, S., 2018. Optimal PI and PID control of first-order plus delay processes and evaluation
674 of the original and improved SIMC rules. J. Process Control 70, 36–46.
675 https://doi.org/10.1016/j.jprocont.2018.06.011

676 Heller, D., Einfalt, D., 2022. Reproducibility of Fruit Spirit Distillation Processes. Beverages 8.
677 https://doi.org/10.3390/beverages8020020

678 Hodel, J., O'Donovan, T., Hill, A.E., 2021. Influence of still design and modelling of the behaviour of volatile
679 terpenes in an artificial model gin. Food Bioprod. Process. 129, 46–64.
680 https://doi.org/10.1016/j.fbp.2021.07.002

681 Holds, H.R., 2023. Brandies, grape spirits, and fruit distillates, First Edit. ed, Distilled Spirits. Elsevier Ltd.
682 https://doi.org/10.1016/B978-0-12-822443-4.00005-0

683 Iannone, R., Miranda, S., Riemma, S., De Marco, I., 2016. Improving environmental performances in wine
684 production by a life cycle assessment analysis. J. Clean. Prod. 111, 172–180.
685 https://doi.org/10.1016/j.jclepro.2015.04.006

686 Knowles, J., 2006. ParEGO: A hybrid algorithm with on-line landscape approximation for expensive
687 multiobjective optimization problems. IEEE Trans. Evol. Comput. 10, 50–66.
688 https://doi.org/10.1109/TEVC.2005.851274

689 Krishnan, A.R., Hamid, M.R., Tanakinjal, G.H., Asli, M.F., Boniface, B., Ghazali, M.F., 2023. An investigation
690 to offer conclusive recommendations on suitable benefit/cost criteria-based normalization methods for
691 TOPSIS. MethodsX 10. https://doi.org/10.1016/j.mex.2023.102227

692 Kumar, S.S., Indiran, T., Itty, G.V., Shettigar J, P., Paul, T.V., 2022. Development of a Nonlinear Model

Predictive Control-Based Nonlinear Three-Mode Controller for a Nonlinear System. ACS Omega 7, 42418–42437. https://doi.org/10.1021/acsomega.2c05542

Kvernland, M., Halvorsen, I., Skogestad, S., 2010. Model Predictive Control of a Kaibel Distillation Column. IFAC Proc. Vol. 43, 553–558. https://doi.org/10.3182/20100705-3-BE-2011.00092

Lin, S., 2011. NGPM -- A NSGA-II Program in Matlab v1.4 [WWW Document]. Matlab Cent. File Exch. URL https://www.mathworks.com/matlabcentral/fileexchange/31166-ngpm-a-nsga-ii-program-in-matlab-v1-4 (accessed 1.19.23).

Lopez-Saucedo, E.S., Grossmann, I.E., Segovia-Hernandez, J.G., Hernández, S., 2016. Rigorous modeling, simulation and optimization of a conventional and nonconventional batch reactive distillation column: A comparative study of dynamic optimization approaches. Chem. Eng. Res. Des. 111, 83–99. https://doi.org/10.1016/j.cherd.2016.04.005

Luna, R., López, F., Pérez-Correa, J.R., 2021. Design of optimal wine distillation recipes using multi-criteria decision-making techniques. Comput. Chem. Eng. 145, 107194. https://doi.org/10.1016/j.compchemeng.2020.107194

Luna, R., López, F., Pérez-Correa, J.R., 2018. Minimizing methanol content in experimental charentais alembic distillations. J. Ind. Eng. Chem. 57, 160–170. https://doi.org/10.1016/j.jiec.2017.08.018

Luna, R., Matias-Guiu, P., López, F., Pérez-Correa, J.R., 2019. Quality aroma improvement of Muscat wine spirits: A new approach using first-principles model-based design and multi-objective dynamic optimisation through multi-variable analysis techniques. Food Bioprod. Process. 115, 208–222. https://doi.org/10.1016/j.fbp.2019.04.004

Manfred Morari, Zafiriou, E., 1989. Robust process control. Prentice-Hall, Englewood Cliffs, USA.

Martins, A.A., Araújo, A.R., Graça, A., Caetano, N.S., Mata, T.M., 2018. Towards sustainable wine: Comparison of two Portuguese wines. J. Clean. Prod. 183, 662–676. https://doi.org/10.1016/j.jclepro.2018.02.057

May-Vázquez, M.M., Gómez-Castro, F.I., Rawlings, E.S., Rico-Ramírez, V., Rodríguez-Ángeles, M.A., 2022. Optimal control of a rate-based modelled batch distillation column: Initialization strategy. Comput. Chem. Eng. 162. https://doi.org/10.1016/j.compchemeng.2022.107811

Meidanshahi, V., Corbett, B., Adams, T.A., Mhaskar, P., 2017. Subspace model identification and model predictive control based cost analysis of a semicontinuous distillation process. Comput. Chem. Eng. 103, 39–57. https://doi.org/10.1016/j.compchemeng.2017.03.011

Monroy-Loperena, R., Alvarez-Ramirez, J., 2000. Output-Feedback Control of Reactive Batch Distillation Columns. Ind. Eng. Chem. Res. 39, 378–386. https://doi.org/10.1021/ie990382l

Muñoz, A.A., Klock-Barría, K., Alvarez-Garreton, C., Aguilera-Betti, I., González-Reyes, Á., Lastra, J.A., Chávez, R.O., Barría, P., Christie, D., Rojas-Badilla, M., Lequesne, C., 2020. Water crisis in petorca basin, Chile: The combined effects of a mega-drought and water management. Water (Switzerland) 12. https://doi.org/10.3390/w12030648

Nemeth, B., Lang, P., Hegely, L., 2020. Optimisation of solvent recovery in two batch distillation columns of different size. J. Clean. Prod. 275, 122746. https://doi.org/10.1016/j.jclepro.2020.122746

Osorio, D., Pérez-Correa, J.R., Biegler, L.T., Agosin, E., 2005. Wine distillates: Practical operating recipe formulation for stills. J. Agric. Food Chem. 53, 6326–6331. https://doi.org/10.1021/jf047788f

Osorio, D., Pérez-Correa, R., Belancic, A., Agosin, E., 2004. Rigorous dynamic modeling and simulation of wine distillations. Food Control 15, 515–521. https://doi.org/10.1016/j.foodcont.2003.08.003

Parhi, S.S., Rangaiah, G.P., Jana, A.K., 2019. Multi-objective optimization of vapor recompressed distillation column in batch processing: Improving energy and cost savings. Appl. Therm. Eng. 150, 1273–1296. https://doi.org/10.1016/j.applthermaleng.2019.01.073

Ramasamy, V., Sidharthan, R.K., Kannan, R., Muralidharan, G., 2019. Optimal tuning of model predictive controller weights using genetic algorithm with interactive decision tree for industrial cement kiln

process. Processes 7. https://doi.org/10.3390/PR7120938

Sacher, J., García-Llobodanin, L., López, F., Segura, H., Pérez-Correa, J.R., 2017. The Spirit World: Can chemical engineering help spirits distillers close the loop between historic roots and modern modelling methods? Chem. Eng. 32–35.

Sacher, J., García-Llobodanin, L., López, F., Segura, H., Pérez-Correa, J.R., 2013. Dynamic modeling and simulation of an alembic pear wine distillation. Food Bioprod. Process. 91, 447–456. https://doi.org/10.1016/j.fbp.2013.04.001

Sarkar, D., Rohani, S., Jutan, A., 2006. Multi-objective optimization of seeded batch crystallization processes. Chem. Eng. Sci. 61, 5282–5295. https://doi.org/10.1016/j.ces.2006.03.055

Scanavini, F., Cassini, C., Souza, E., F., M., Meirelles, A., 2010. Cachaça production in a lab-scale alembic: Modeling and computational simulation. J. Food Process Eng. 33, 226–252. https://doi.org/10.1111/j.1745-4530.2008.00352.x

Schiesser, W.E., Griffiths, G.W., 2009. A Compendium of Partial Differential Equation Models: Method of Lines Analysis with Matlab. Cambridge University Press, New York, US.

Silva, W.C., Araújo, E.C.C., Calmanovici, C.E., Bernardo, A., Giulietti, M., 2017. Environmental assessment of a standard distillery using aspen plus®: Simulation and renewability analysis. J. Clean. Prod. 162, 1442–1454. https://doi.org/10.1016/j.jclepro.2017.06.106

Skogestad, S., 2004. Simple analytic rules for model reduction and PID controller tuning. Model. Identif. Control 25, 85–120. https://doi.org/10.4173/mic.2004.2.2

Soares, A.M., Henderson, N., Mota, B.T., Pires, A.P., Ramos, V.D., 2019. A new pot still distillation model approach with parameter estimation by multi-objective optimization. Comput. Chem. Eng. 130, 106570. https://doi.org/10.1016/j.compchemeng.2019.106570

Spaho, N., 2017. Distillation Techniques in the Fruit Spirits Production. Distill. - Innov. Appl. Model. https://doi.org/10.5772/66774

Sridhar, L.N., 2020. Multiobjective nonlinear model predictive control of pharmaceutical batch crystallizers. Drug Dev. Ind. Pharm. 46, 2089–2097. https://doi.org/10.1080/03639045.2020.1847135

Tarafder, A., Rangaiah, G.P., Ray, A.K., 2007. A study of finding many desirable solutions in multiobjective optimization of chemical processes. Comput. Chem. Eng. 31, 1257–1271. https://doi.org/10.1016/j.compchemeng.2006.10.010

Tenorio, L.M.S., Batista, F.R.M., Monteiro, S., 2023. Non-Conventional Cuts in Batch Distillation to Brazilian Spirits (cachaça) Production: A Computational Simulation Approach. Processes 11. https://doi.org/10.3390/pr11010074

Valderrama, J.O., Toselli, L.A., Faúndez, C.A., 2012. Advances on modeling and simulation of alcoholic distillation. Part 2: Process simulation. Food Bioprod. Process. 90, 832–840. https://doi.org/10.1016/j.fbp.2012.04.003

Völker, M., Sonntag, C., Engell, S., 2007. Control of integrated processes: A case study on reactive distillation in a medium-scale pilot plant. Control Eng. Pract. 15, 863–881. https://doi.org/10.1016/j.conengprac.2006.03.002

White, J.S., 2023. Sustainable distilling: CO2 emissions, energy decarbonization, and by-products, First Edit. ed, Distilled Spirits. Elsevier Ltd. https://doi.org/10.1016/B978-0-12-822443-4.00011-6

Wilson, D.I., Young, B.R., 2006. The Seduction of Model Predictive Control. Electr. Autom. Technol. 27–28.

Yaghoubzadeh-Bavandpour, A., Bozorg-Haddad, O., Zolghard-Asli, B., Reza-Nikoo, M., 2022. Computational Intelligence for Water and Environmental Sciences. Springer Nature Singapore, Warsaw, Poland.